Experimental antiproton nuclear stopping power in H_2 and D_2

A. Bertin, M. Bruschi, M. Capponi, I. D'Antone, S. De Castro, A. Ferretti, D. Galli, B. Giacobbe, U. Marconi, M. Piccinini, N. Semprini Cesari, R. Spighi, S. Vecchi, A. Vezzani, F. Vigotti, M. Villa, A. Vitale, and A. Zoccoli
Dipartimento di Fisica, Università di Bologna, and Istituto Nazionale di Fisica Nucleare Sezione di Bologna, Bologna, Italy

M. Corradini, A. Donzella, E. Lodi Rizzini, and L. Venturelli
Dipartimento di Chimica e Fisica per i Materiali, Università di Brescia and Istituto Nazionale di Fisica Nucleare Sezione di Torino, Brescia, Italy

A. Zenoni
Dipartimento di Chimica e Fisica per i Materiali, Università di Brescia and Istituto Nazionale di Fisica Nucleare Sezione di Pavia, Brescia, Italy

C. Cicalò, A. Masoni, G. Puddu, S. Serci, P. Temnikov, and G. L. Usai
Dipartimento di Scienze Fisiche, Università di Cagliari, and Istituto Nazionale di Fisica Nucleare Sezione di Cagliari, Cagliari, Italy

V. G. Ableev, O. Yu Denisov, O. E. Gorchakov, S. N. Prakhov, A. M. Rozhdestvensky, M. G. Sapozhnikov, and W. Tretyak
Joint Institute for Nuclear Research, Dubna, Moscow, Russia

M. Poli
Dipartimento di Energetica, Università di Firenze and Istituto Nazionale di Fisica Nucleare, Sezione di Bologna, Bologna, Italy

P. Gianotti, C. Guaraldo, A. Lanaro, V. Lucherini, F. Nichitiu* C. Petrascu,* and A. Rosca*
Laboratori Nazionale di Frascati dell' Istituto Nazionale di Fisica Nucleare, Frascati, Italy

C. Cavion, U. Gastaldi, M. Lombardi, L. Vannucci, and G. Vedovato
Laboratori Nazionale di Legnaro dell' Istituto Nazionale di Fisica Nucleare, Legnaro, Italy

M. Morando and R. A. Ricci
Dipartimento di Fisica, Università di Padova and Istituto Nazionale di Fisica Nucleare Sezione di Padova, Padova, Italy

G. Bendiscioli, V. Filippini, A. Fontana, P. Montagna, A. Rotondi, A. Saino, and P. Salvini
Dipartimento di Fisica Nucleare e Teor., Università di Pavia and Istituto Nazionale di Fisica Nucleare Sezione di Pavia, Pavia, Italy

F. Balestra, E. Botta, T. Bressani, M. P. Bussa, L. Busso, D. Calvo, P. Cerello, S. Costa, A. Feliciello, L. Ferrero, R. Garfagnini, A. Grasso, A. Maggiora, S. Marcello, D. Panzieri, D. Parena, E. Rossetto, F. Tosello, and G. Zosi
Istituto di Fisica, Università di Torino and Istituto Nazionale di Fisica Nucleare Sezione di Torino, Torino, Italy

A. Filippi
Dipartimento di Fisica Nucleare e Teor., Università di Pavia and Istituto Nazionale di Fisica Nucleare Sezione di Torino, Torino, Italy

M. Agnello, F. Iazzi, and B. Minetti
Politecnico di Torino and Istituto Nazionale di Fisica Nucleare Sezione di Torino, Torino, Italy

G. Pauli and S. Tessaro
Istituto di Fisica, Università di Trieste and Istituto Nazionale di Fisica Nucleare Sezione di Trieste, Trieste, Italy

L. Santi
Dipartimento di Fisica, Università di Udine and Istituto Nazionale di Fisica Nucleare Sezione di Trieste, Udine, Italy

(Received 16 July 1996)

Data about antiprotons slowing down in gaseous targets at very low energies ($E<1$ keV) show that the stopping power in D_2 is lower than in H_2; the right way to explain this behavior seems to be through a nuclear stopping power derived from the classical Rutherford formula. [S1050-2947(96)09312-2]
PACS number(s): 34.50.Bw

*On leave from Dept. of High Energy Physics, Inst. of Atomic Physics, Bucharest, Romania.

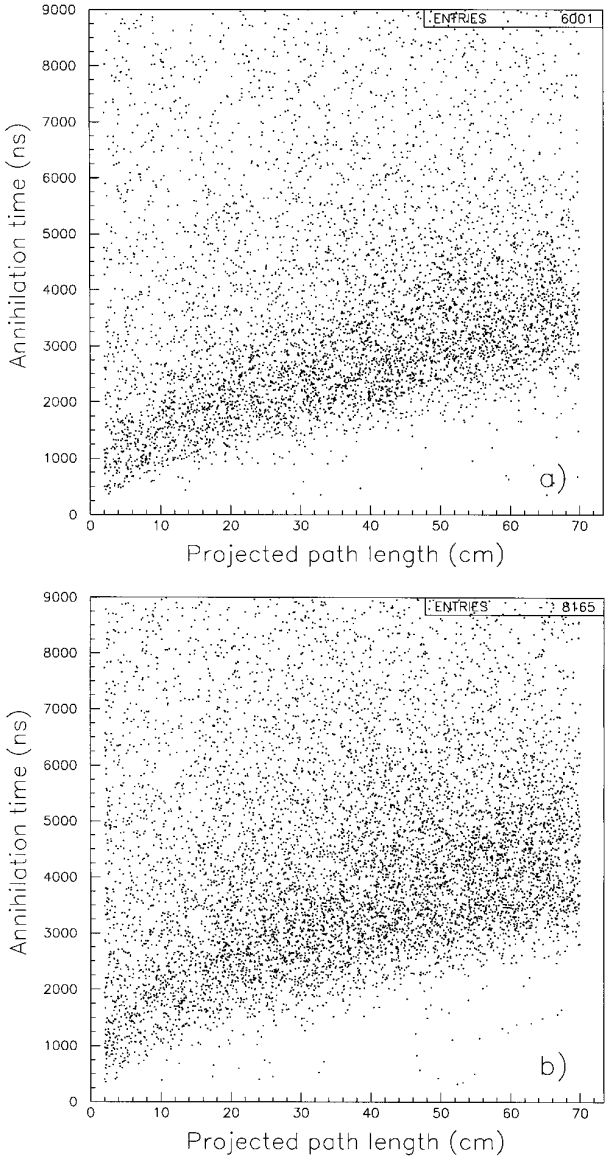

FIG. 1. (a) experimental annihilation times vs projected path length in H_2 at 0.2 mb. The first two centimeters were cut to eliminate window background. (b) the same for D_2.

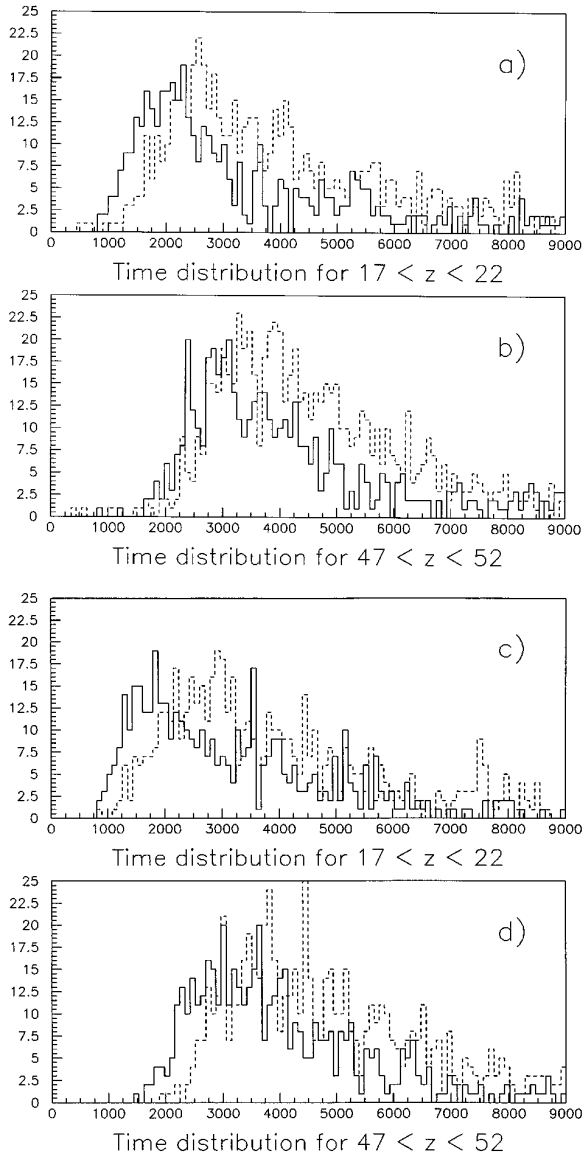

FIG. 2. Experimental (a),(b) and Monte Carlo (c),(d) slices in the distributions of Figs. 1 and 5 for 5 cm wide bins at different points of the target. Dotted: D_2. Solid: H_2.

Starting from the fundamental work of Bohr [1], in the Bethe theory and its several extensions [2–7] the energy loss per unit path length (or stopping power) of a charged particle in traversing matter is explained mainly by the interaction with the electrons of the target atoms or molecules resulting in excitation and/or ionization. In the following this mechanism will be called the electronic stopping power (ESP). The correctness of the theoretical approach was confirmed by many experimental data.

On the other hand, in the case of heavy particles (like $\overline{p}$) at very low speed (much less than the electron velocity $e^2/\hbar$) the electronic contribution to the energy loss becomes much less important and the major contribution to the slowing down is supposed to be due to collisions with atomic nuclei. This mechanism has been called nuclear stopping power (in the following NSP) and, while several models and estimates [6,8–11] exist, up to now few experimental data were available to check their validity. In a previous work [12] we found that, in order to reproduce our experimental data on the stopping power for $\overline{p}$ in H_2 and He between 0.5 and 1.1 keV, it was necessary to introduce an increase of the SP for $\overline{p}$ below 500 eV, not accounted for by ESP. Though we had a little sensitivity at these low energies, it was interpreted as an indication of the presence of some NSP. Now we present a set of data which show clear evidence for a ''nuclear term'' in the stopping power.

The experimental setup of the OBELIX apparatus at CERN [13] lets the $\overline{p}$ from LEAR (Low-Energy Antiproton Ring), degraded by a suitable thickness of mylar, enter a gaseous target with their energy continuously distributed from a maximum to zero. The target (useful length = 75 cm, diameter = 22 cm) was filled with H_2 or D_2 at 0.2 mbar pressure. As explained in Refs. [12] and [13], our apparatus allows us to identify annihilations and to measure the annihilation time (related to the incoming $\overline{p}$ signal) as well as the vertex coordinates of each event. In Figs. 1(a) and 1(b) every point represents the position (z is the depth into the target) and the time at which an annihilation at rest took place in the

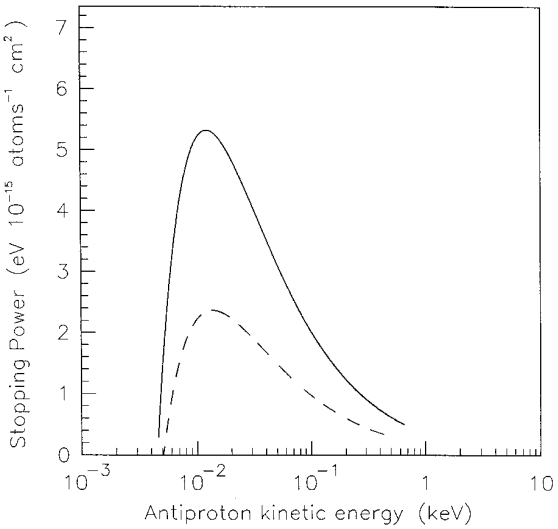

FIG. 3. Curves of the nuclear stopping power obtained by the Rutherford cross section with minimum transfered energy equal to the binding energy of the molecules. Dashed: D_2. Solid: H_2.

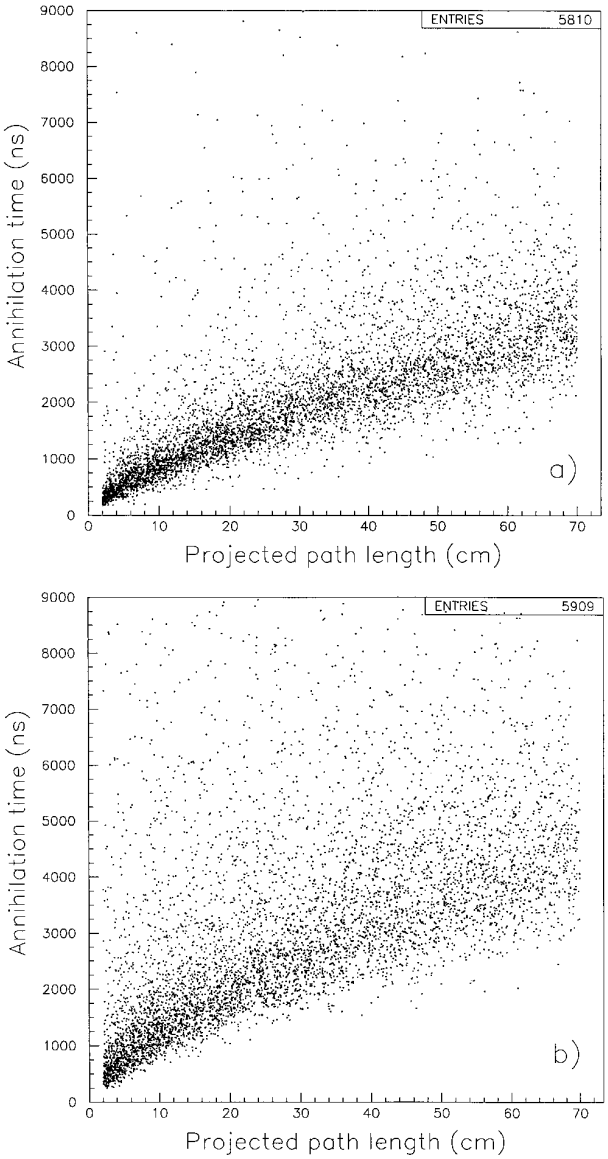

FIG. 4. (a) Monte Carlo simulation for H_2 at 0.2 mb according to classical Rutherford scattering. (b) the same for D_2.

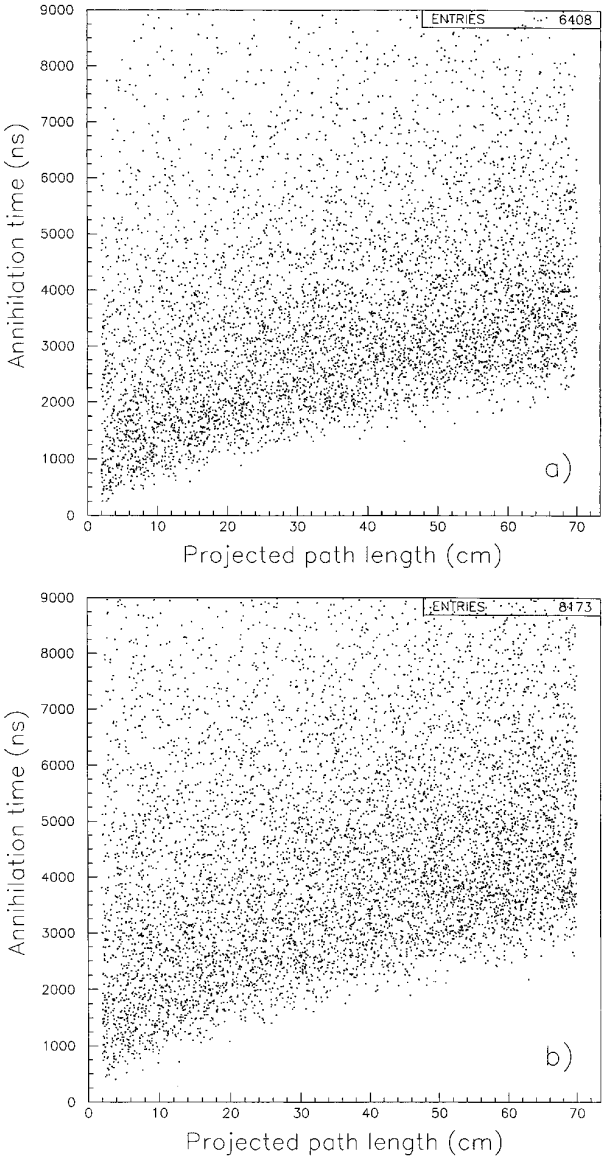

FIG. 5. (a) Monte Carlo simulation for H_2 at 0.2 mb obtained with NSP + ESP plus a cascade time distribution with a mean lifetime of 2.1 μs. (b) the same for D_2, with a mean lifetime of 2.8 μs.

gas. This time is the sum of the deceleration time (which decreases as the stopping power increases) and the deexcitation cascade time. As can be seen, the annihilation points accumulate mainly along a band close to the lower edge of the distribution, and the positions of the accumulation bands, essentially determined by the stopping power, is different for H_2 and D_2. The difference is even more evident in Figs. 2(a) and 2(b) which show the time distributions of the annihilation points in 5 cm wide bins for $17<z<22$ and for $47<z<52$ cm, for both the gases. For a given z interval, the annihilation time is on the average lower in H_2 than in D_2, meaning that the stopping power is stronger in H_2. The point spread in time above the accumulation band is due mainly to the cascade time at low density (see below).

Due to the fact that the electronic structure of the two gases is practically the same, a first conclusion might be that the difference in the accumulating bands is mainly due to

NSP. To show this, we proceeded in steps. First we simulated the annihilation time vs the projected path length considering for the stopping power the expression obtained extrapolating our previous data [12], which accounts essentially for ESP. As at low projectile velocities the difference between the real path length and the projected path length (i.e., the z coordinate that we measure) may be significant, we considered the angular deviations along the path due to the nuclear scattering according to the Rutherford cross section $d\sigma=\pi(Z_1Z_2e^2/mv_\infty^2)^2[\cos(\theta/2)/\sin^3(\theta/2)]\,d\theta$. The behavior of the accumulation band for H_2 results very different from the experimental one (in particular, the annihilation times are too high), so confirming that now the main energy loss is not due to ESP.

In the simulation of a NSP we used the simplest model, i.e., the classical Rutherford scattering, limiting the minimum transferred energy to the binding energy of the target molecule, $\frac{1}{3}(e^2/2a_0)$, as suggested by Wightman [10]. Since the scatterer and the scattered particle have similar masses, recoil effects and the transformations between center of mass and laboratory systems were taken into account [14,15]. NSP of H_2 and D_2 are shown in Fig. 3. The mean energy of antiprotons with a range equal to the useful target length turns out to be about 600 eV for H_2 and 400 eV for D_2.

Figures 4(a) and 4(b) show that the behavior of the accumulation bands is rather well reproduced but the annihilation times are somewhat smaller than in the experimental scatter plots [Figs. 1(a) and 1(b)], and the points above the bands are less spread than in the experimental case. This difference may be accounted for by reminding that the antiproton annihilation is preceded by the formation of $\overline{pp}$ atoms [16,17]. They may deexcite from many atomic levels and at very low densities the actual cascade time is the result of several exponential decays. As we were interested only in its order of magnitude we considered just one exponential function with a mean lifetime to be determined by fitting the experimental scatter plots. Finally we simulated the data considering ESP, NSP, and cascade time altogether. As shown in Figs. 5(a) and 5(b) and 2(c) and 2(d) this approach reproduces the data satisfactorily with mean lifetimes of the captured antiprotons of 2.1 μs for H_2 and 2.8 μs for D_2. These values are consistent with the theoretical predictions [17] and our previous results [18].

The comparison among Figs. 1, 2, and 5 shows that experimental data and Monte Carlo simulations are in fairly good agreement, allowing us to draw the following conclusions: (i) the electronic stopping power, by itself, is not able to explain the differences observed between the stopping power in H_2 and D_2 (even if its rise at low energies is taken into account, as suggested by Dolinov *et al.* [19]; (ii) the main part of such a difference may be explained only through the introduction of a nuclear stopping power, already by a very simple model as the bare Rutherford's one; (iii) the annihilation of antiprotons is preceded by the formation of protonium, with a cascade time similar to that which we can extrapolate by the existing data at higher target densities.

Actually, several effects [20,21] are supposed to come into play with different weights when we are dealing with very low energies and low atomic numbers, such as the screening of the Coulomb field by the atomic electrons, the finite size of the scattering nucleus, the contribution to the total scattering by atomic electrons, spin effects, quasimolecular effects, etc. It must be underlined also that positive and negative projectiles need a different theoretical treatment [10,22]. Antiprotons proved to be the ideal projectiles for this type of investigation but we would emphasize that only working at very low pressures with the possibility of a good reconstruction of the spatial and temporal coordinates of the annihilation events was it possible to obtain such experimental evidence of nuclear stopping power.

[1] N. Bohr, Philos. Mag. **25**, 10 (1913).
[2] H. A. Bethe, Ann. Phys. (Leipzig) **5**, 325 (1930).
[3] F. Bloch, Ann. Phys. (Leipzig), **16**, 287 (1933).
[4] W. H. Barkas, J. N. Dyer, and H. H. Heckman, Phys. Rev. Lett. **11**, 26 (1963).
[5] M. Inokuti, Rev. Mod. Phys. **43**, 297 (1971).
[6] J. F. Ziegler, J. P. Biersack, and U. Littmark, *The Stopping and Range of Ions in Solids* (Pergamon, Oxford, 1985).
[7] H. Knudsen and J. F. Reading, Phys. Rep. **212**, 107 (1992).
[8] J. Lindhard, M. Scharff, and H. E. Schiøtt, Videnk. Selsk. Mat. Fys. Medd. **33** (14) (1963).
[9] S. Kalbitzer *et al.*, Z. Phys. A **278**, 223 (1976).
[10] A. S. Wightman, Phys. Rev. **77**, 521 (1950).
[11] W. D. Wilson, L. G. Haggmark, and J. P. Biersack, Phys. Rev. B **15**, 2458 (1977).
[12] M. Agnello *et al.*, Phys. Rev. Lett. **74**, 371 (1995).
[13] A. Adamo *et al.*, Nucl. Phys. A **558**, 665 (1993).
[14] E. V. Hungerford *et al.*, Nucl. Phys. A **197**, 515 (1972).
[15] G. Bendiscioli *et al.*, Nuovo Cimento A **68**, 101 (1982).
[16] G. T. Condo, Phys. Lett. **9**, 65 (1964).
[17] G. Reifenröther and E. Klempt, Nucl. Phys. A **503**, 885 (1989).
[18] A. Adamo *et al.*, Phys. Lett. B **285**, 15 (1992).
[19] V. K. Dolinov *et al.*, Muon Catalyzed Fusion **4**, 169 (1989).
[20] W. T. Scott, Rev. Mod. Phys. **35**, 231 (1963).
[21] R. Golser and D. Semrad, Phys. Rev. Lett. **66**, 1831 (1992).
[22] D. L. Morgan, Jr., Hyperfine Interact. **44**, 399 (1988).